



Aerodynamic Analysis of Unnamed Aerial Vehicle Serindit V-2 Using Computational Fluid Dynamics

Asral^{1,*}, Kaspul Anuar¹, Agung Soegihin¹

¹ Department of Mechanical Engineering, Engineering Faculty, Universitas Riau, Kampus Bina Widya Jl. HR. Soebrantas Km 12,5 Simpang Baru, Panam, Pekanbaru 28293, Indonesia

ARTICLE INFO

Article history:

Received 26 September 2021

Received in revised form 16 January 2022

Accepted 23 January 2022

Available online 5 March 2022

Keywords:

Aircraft; angle of attack; UAV; aerodynamics

ABSTRACT

Serindit V-2 is an unnamed aircraft by the Serindit Aero UAV research team. It has the ability to fly rapidly in order to compete in KRTI in the Racing Plane division. Although it has been successfully produced and able to fly, comprehensive research on aerodynamic of Serindit V-2 aircraft flying behavior has never been done before. Aerodynamic research needs to be conducted to improve the aircraft performance such as flying capability, air resistance efficiency and etc. This study aims to determine the value of flow characteristic such as coefficient of drag, lift, moment and pressure distribution based on fluid flow that occurs in the aircraft with variations of Angle of Attack and air velocity. The method used is CFD (Computational Fluid Dynamic) which is a computer-based numerical method and performed with an iterative procedure to predict aerodynamic characteristics and fluid flow phenomena on the aircraft surface. Simulations were carried out using Ansys Fluent 2017 software on the Serindit V-2 aircraft model sourced from the Serindit Aero Team. The result of the lift coefficient value is $C_{L\alpha}=0.3666$ and $C_{L_{MAX}}$ value = 1.42626 at $\alpha 13^\circ$. The $C_{D\alpha}$ obtained was 0.0589258. While the C_{Mo} value obtained is -8.34×10^{-5} .

1. Introduction

Unnamed Aerial Vehicle (UAV) is a vehicle for unnamed flying object that can be controlled manually or autonomously which in the last decade has grown rapidly in the realm of unmanned systems research in the world [1,2]. To develop this innovation and technology, the Director General of Belmawa, Kemenristekdikti create KRTI (Indonesian Flying Robot Competition). As a form of participation and pioneering research, the Department of Mechanical Engineering, Riau University has formed a UAV Serindit Aero research team. In the KRTI Racing Plane division, as can be seen in Figure 1. A vehicle is required to be able to take off in a limited area, fly quickly to reach the desired location safely and accurately on a predetermined path, and be able to land safely again. Its application is in special missions such as rescue which require the ability to fly fast. Either complex or simple, the principle of force and moment of an object lies only in two manners such as pressure distribution and shear stress distribution on object's surface. Both the pressure, p and the shear

* Corresponding author.

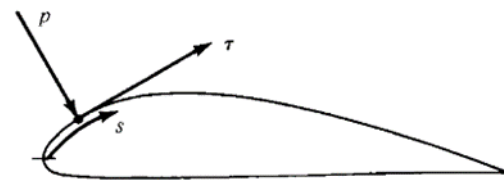
E-mail address: asral@lecturer.unri.ac.id

<https://doi.org/10.37934/arfmts.93.1.8393>

stress, τ have dimensions of force per surface area. As seen in Figure 2, p works normally to the surface of the object, while τ works tangentially. Shear stress occurs due to the effect of pulling on the surface of the object caused by the friction force between the surface and the air [3].



Fig. 1. Serindit V-2 aircraft [4]



$p = p(s)$ = surface pressure distribution
 $\tau = \tau(s)$ = surface shear stress distribution

Fig. 2. Pressure and shear stress on surface [3]

By assuming incompressible flow or no changes in density, if ρ_∞ is airflow density and V_∞ is airflow velocity, therefore dynamic pressure, q could be defined as [5,6].

$$q_\infty = \frac{1}{2} \rho_\infty V_\infty^2 \quad (1)$$

Dynamic pressure has the same units as pressure in general (lb/ft² or N/m²). In addition, S is the area and l is the length, so the force and moment coefficients can be defined as follows

$$C_L = \frac{L}{q_\infty S} \quad (2)$$

$$C_D = \frac{D}{q_\infty S} \quad (3)$$

$$C_M = \frac{M}{q_\infty S l} \quad (4)$$

When a fluid flows on the surface of an object, an air flow pattern affects the force and pressure acting on the object. The flow patterns of laminar and turbulent fluids depend on the geometric shape, surface roughness, air flow velocity, surface temperature, and the type of fluid flowing. Osborne Reynold found that the air flow pattern occurs based on the ratio of the inertial force to the viscous force. This ratio is known as the Reynold Number [7].

$$Reynold\ Number = \frac{\rho \times v \times l}{\mu} \quad (5)$$

The aerodynamic analysis of an aircraft is very important and has been carried out by several researchers [8-10]. One of the studies analyzes the stress distribution on the airfoil surface of an aircraft wing [11]. It can be seen through a simulation that at the top of the wing, the pressure will be lower than the underside of the wing. And the projection area with high pressure below the airfoil will increase along with the increase in the angle of attack [12].

Pinindriya in 2013 also performed aerodynamic simulations of the LSU 05 drone to find the C_L , C_D and C_M values [13]. According to her, the plane begins to lose its lift when it reaches a certain angle of attack. Marked by the value of C_L which decreases after reaching the point of the maximum value of C_L . The condition in which an airplane loses its lift force is called a stall [14].

Computational Fluid Dynamic (CFD) is a computer-based analysis system to simulate the behavior of a system involving fluid flow, heat transfer and other physical processes. How it works by solving fluid flow equations (in a certain form) covering a desired area, with conditions at the boundaries of the area are specific and known [15]. CFD is arranged in such a way based on a numerical algorithm to solve a problem. Many CFD software are equipped with powerful interfaces to be able to input various problem parameters to be solved [16,17]. In general, there are three main processes in using CFD analysis, including: pre-processor, processing / solver, post-processor [18,19].

2. Methods

On the process of simulation, Ansys Fluent 2017 software is used. There are three stages of the process. Simulations will be carried out repeatedly according to the research variables. The variables are angle of attack variation and airflow speed variation. The result of the simulation will be the data of drag, lift and moment coefficients; data of pressure distribution on the aircraft surface. The simulation results will also be presented through graphs and contour visualization. The first stage of the simulation is pre-processing. In this stage geometry modeling is carried out on the Serindit V-2 aircraft design to create an additional domain as a representation of a wind tunnel. At this pre-processing stage, the meshing process is also carried out.

To determine the suitable configuration of Mesh, Grid Independency Test is carried out by using the number of element variation. The Parameter is C_L which resulted by every mesh variation. The variation are ranged between $\pm 1.000.000$ – $\pm 1.500.000$ elements on every mesh type, as in Table 1. There are two criteria to determine which meshing type will be used, such error percentage and iteration time.

Table 1

Mesh type	
Mesh type	Element
Very coarse	$\pm 1.000.000$
Coarse	$\pm 2.000.000$
Normal	$\pm 3.000.000$
Fine	$\pm 4.000.000$
Very fine	$\pm 5.000.000$

Mesh sizes are configured repeatedly to match the number of elements of mesh types. There are three ways to configure mesh size such as sizing type of Body Influence, face Sizing with size plane surface and the inflation on plane surface. The domain model are labelled on each side by using the “named selection” configuration. This is important because it will be used to input the boundary condition.

The second stage is Processing/Solution. At this stage all values, variables, conditions, solution methods, turbulent models, and other configurations are submitted to the solver to create a condition that represents the actual nature as close as possible. Solution Method and iteration settings are configured before the computer generate the simulation values required for further data analysis. The details of the fluent solver setup shown in Table 2.

The third stage of the simulation is Post Processing. After the iteration is done on the solver, the simulation results are taken. Data such as force, coefficient, pressure, velocity, graph curves, and visualization of flow profile are collected.

Table 2
 Solver setup

Setup	Detail
General setup	3 Dimension, pressure based, steady
Turbulent model	K- Epsilon (2 eqn) – Realizable, std wall function
Material	Fluid (Air) (Density = 1.2041 kg/m ³)
Boundary condition	Inlet – Velocity inlet Body – Wall Outlet – Pressure outlet Symmetry - Symmetry Top, side, bottom - Wall
Airflow speed	12, 16, 20, 26 m/s
Angle of Attack	-5°, -1°, 0°, 1°, 3°, 5°, 7°, 9°, 11°, 13°, 15°, 17°
Solution method	SIMPLEC, Least squares cell based gradient, second order pressure, second order upwind momentum
Solution initialization	Hybrid initialization

2.1 Geometry and Modelling

Table 3 shown the specification of the Serindit V-2 aircraft obtained from the Team work.

Table 3
 Serindit V-2 Specification

Specification	Details
Wing aifoil	MH 30
Tail airfoil	NACA 0010
Wing type	Fixed wing
Fuselage length	1060 mm
Wingspan	1300 mm
Motor system	Brushless motor
Fuselage material	Fiberglass composite
Wing material	Foam core composite
MTOW	2.5 kg

In this study, the design of the aircraft was made using Solidworks 2017, as in Figure 3. Then, the design is exported to Ansys Fluent 2017 for the computational processing. The design has been simplified to ease the meshing process by integrating the surface of the aileron, elevators and rudder with their respective wing or tail sections. We assume the wings, horizontal and vertical tail sections are having no flap and aileron deflection (deflection = 0°). Simulations were carried out on half body of the Serindit V-2 to reduce computational costs. The simulation results will not be disrupted, because it uses a symmetry feature that is recognized by the Ansys Fluent system. So it is as if the simulation is carried out on one fuselage, but with a lower computational cost.

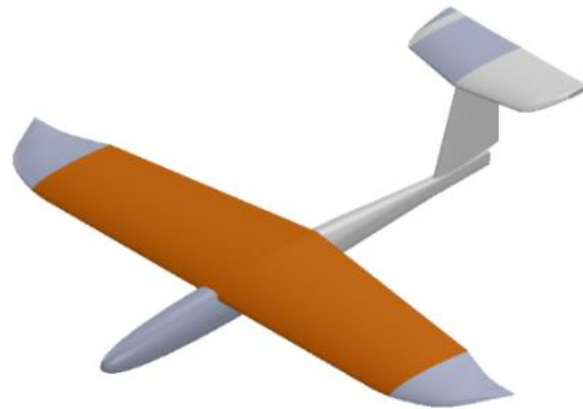


Fig. 3. Geometry of Serindit V-2

Figure 4 shows the dimensional design of the geometric domain used in this study. It represents a virtual wind tunnel where there is an air flow that enters through one side of the domain in the form of an inlet and moves out to the other side which is an outlet. The domain has a symmetry side which is designated as the boundary condition as a plane that mirrors the half of the model. This means that the phenomenon or simulation treatment is equivalent to half of the model. The effect of zero slip or surface shear force on walls, velocity, and other physical phenomena is equal to zero.

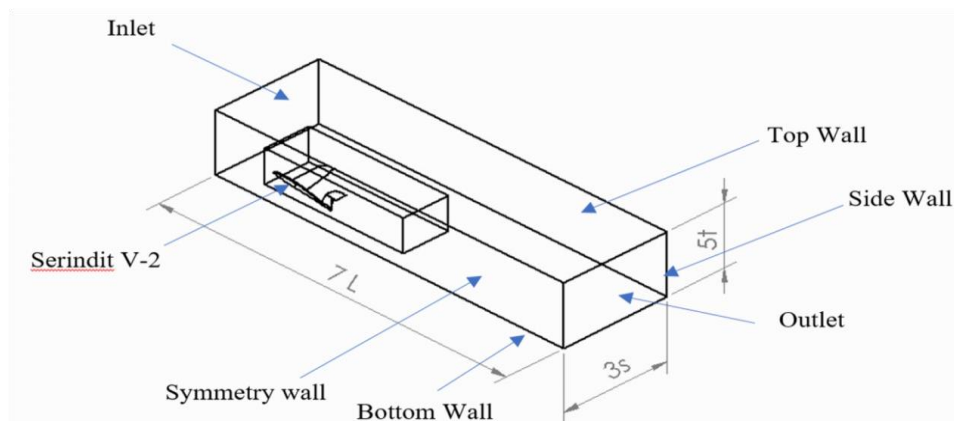


Fig. 4. Domain geometry

where,

L = The length of the plane (1097 mm)

S = $\frac{1}{2}$ Wingspan (664 mm)

T = The height of the plane (239 mm)

2.2 Data Validation

This study done which the geometric model or object being tested is exclusive, which mean an object that hasn't been tested before. Because the information regarding the object design, was only owned and known by the Riau University flying robot team, so it was impossible for outsiders to do so. However, the type and method of this typical of research have been carried out by many researchers.

The wing of the LSU 05 LAPAN aircraft as shown in Figure 5 using CFD with Ansys Fluent software and validated experimentally within Wind Tunnel [20]. Therefore, we will also simulate the wing of LSU 05 LAPAN aircraft. The validation was carried out by testing the geometry of the LSU 05 LAPAN

aircraft wing using a simulation work step on the Serindit V-2 aircraft. Then, the results of the simulation will be compared with the results of experimental data. The work steps that have been validated will be reflected in the results of a parametric comparison against the Romadhon's. When the results are not ideal enough, then the simulation work steps need to be revised again by means of repeated reconfiguration of the mesh and fluid solutions until the value can be claimed as sufficiently resemblant. The LSU 05 aircraft wing geometry shown in Table 4.

Table 4
LSU 05 aircraft wing details [11]

Parameter	Detail
Wing span	5,5 m
Luas sayap	3,246 m ²
Chord root	0,714 m
Chord tip	0,44 m
Airfoil	NACA 4415

In addition to validating through related research, prediction of the Serindit V-2 aircraft simulation results was also carried out using the airfoiltools.com data reference in the form of C_L vs α curves on the MH30 airfoil. To determine a relevant prediction for this study, Reynold Number value was calculated using Eq. (5). This prediction can provide information about curve trends that can be obtained from the simulation results of the Serindit V-2 aircraft. With $Re = 514,629$ the predicted C_L vs α curve on an MH30 airfoil is seen in Figure 6.

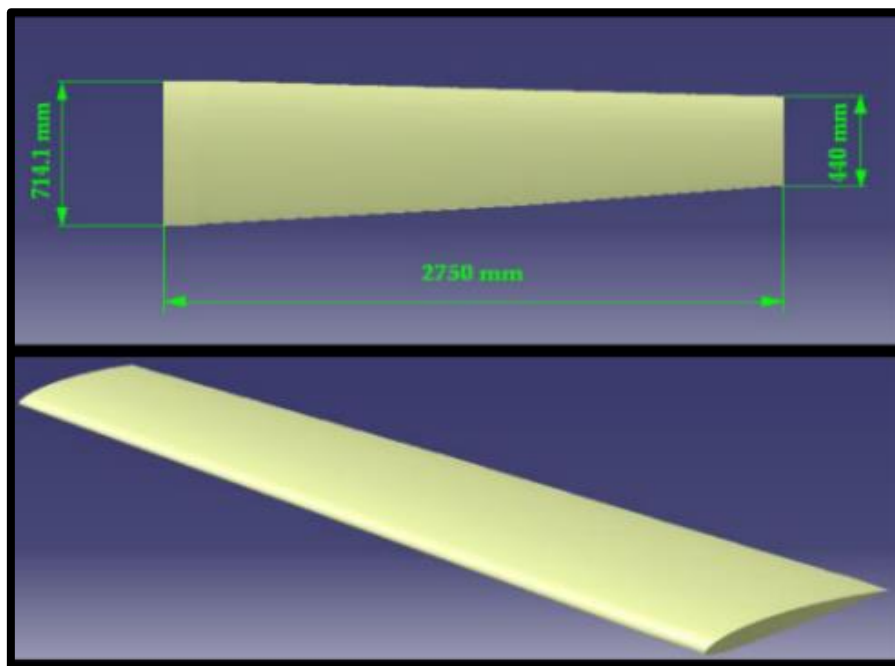


Fig. 5. LSU 05 LAPAN wing geometry

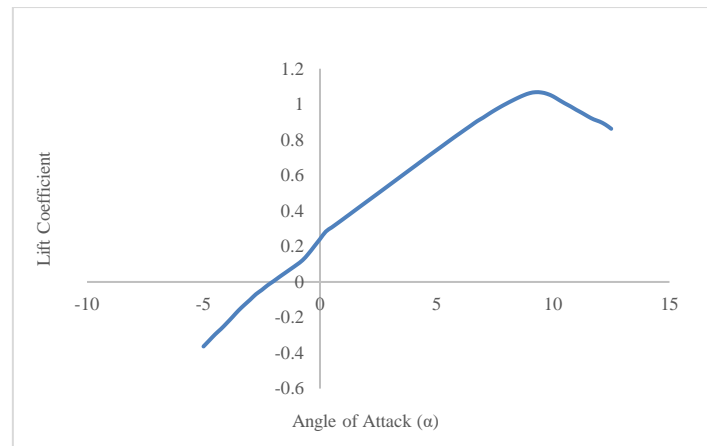


Fig. 6. Prediction of C_L Vs α of airfoil MH30 [14]

3. Result and Discussion

3.1 Grid Independence Test

Grid Independence Test is a process to determine the optimal number and structure of grids and mesh in order to obtain accurate data. The result shown in Table 5 and illustrated in Figure 7.

From Table 5, it can be seen that the mesh variations show relatively similar C_{L0} values, namely in the range of values 0.364 - 0.368. Percentage error is the percentage difference of C_{L0} in each mesh type to the average C_{L0} of all mesh types. So that the selected mesh type is the type that has the smallest percentage Error. Because it represents the overall value of the Grid Independence Test with the smallest percentage Error. The parameters for selecting the mesh type are the percentage error and the iteration time. Therefore, the selected mesh type is coarse because it has the smallest percentage error of 0.00045 % and the iteration time is shorter than the majority of mesh types, which is 31 minutes.

Table 5
 Grid independence assessment on Serindit V-2

Mesh type	Number of element	C_{L0} Serindit	Time (Minute)	% Error
Very Coarse	1.170.555	0.364257	26	0.00511
Coarse	1.923.204	0.366296	31	0.00045
Normal	2.328.676	0.366634	41	0.00137
Fine	3.838.894	0.365908	62	0.00060
Very Fine	6.311.939	0.367561	114	0.00390

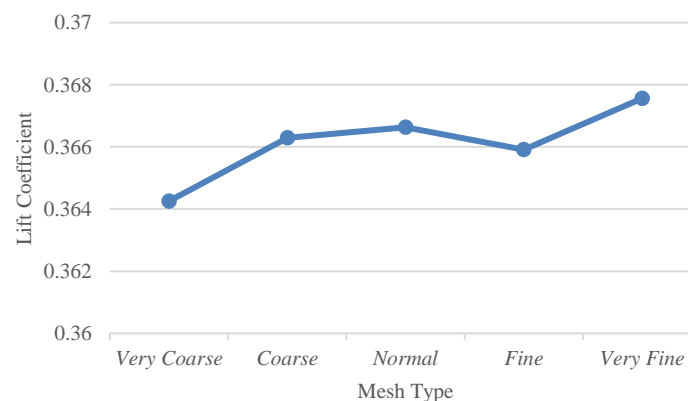


Fig. 7. Grid independence test

3.2 Data Validation

The following data is a parametric comparison of the simulation result towards the result of Romadhon's study (2017). Table 6 shows the percentage error of C_{L0} at the 0° angle of attack. According to the results, the obtained percentage error is quite small, 2.6% for the C_{L0} , which means it is still below than 3%.

Table 6
 Comparison of computation and Romadhon's study

Parameter	Computation (This study)	Romadhon (WT test)	Percentage Error (%)
C_{L0}	0.540883	0.555	2.6

The computation work step process can represent experimentally, due to produce a similar value as seen in Figure 8. From Figure 8 shown that there is a clear difference between the calculation and prediction values. On the initial prediction curve, C_L is relatively lower than the simulation. In addition, the initial prediction curve shows the stall happens at 9° angle of attack while the simulation results at 13° . This difference occurs because in the simulation, the geometric object has more complex part and allow it to produce higher lift. Such as a large wing surface and aircraft elevators which can also generate lift. However, at 0° angle of attack the prediction curve shows a C_L value of 0.2415 while the simulation curve is 0.366766 which can be said to be relatively similar because it is in the range 0.2 - 0.4% of differences. This predictive information is very helpful in the early phases of the study to do a simulation starting at 0° angle of attack. So that it can be continued to take simulation results at other variations of the angle of attack.

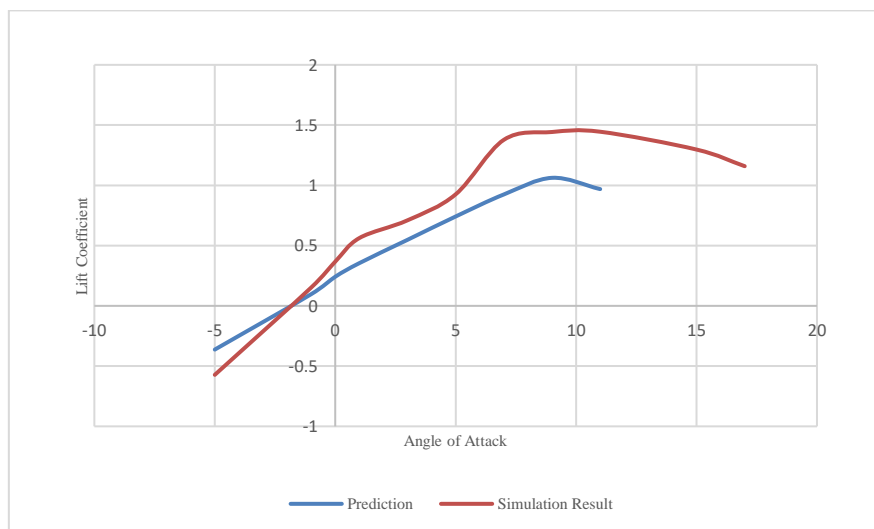


Fig. 8. C_L comparison to MH30 airfoil

3.3 Result on Serindit V-2-Aircraft

Figure 9 shows Lift coefficient At 26 m/s, the aircraft stalled when the plane was oriented with an Angle of Attack 13° . The C_L obtained was 1.42626. It is marked by a curve line that decline after passing $13^\circ \alpha$. This shows that in this form of aircraft orientation, the plane has reached the maximum limit to fly higher. Marked by the lift coefficient at $15^\circ \alpha$ which is smaller than the $13^\circ \alpha$, which is 1.29722. The lift coefficient value is also influenced by the amount of airflow speed. Higher airflow

velocity create higher C_L . As seen in Figure 10. C_L value at $13^\circ \alpha$. At a speed of 12 m/s the C_L is 1.4 and at a speed of 26 m/s it is 1.4262.

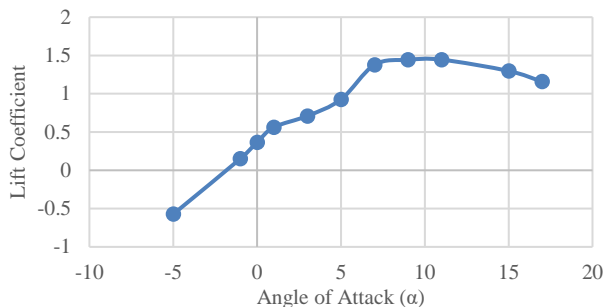


Fig. 9. C_L at air flow 26 m/s

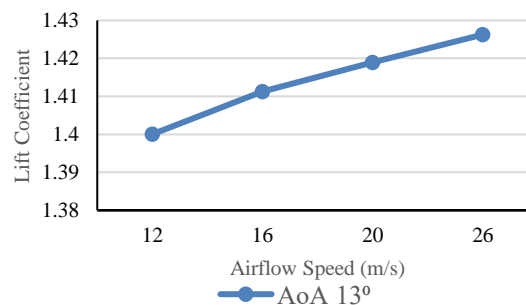


Fig. 10. Airflow effect on coefficient of Lift, C_L

The drag coefficient obtained has experienced an inclining trend. From $0^\circ \alpha$ with $C_D = 0.0589$ to the $17^\circ \alpha$ with $C_D = 0.3099$, as in Figure 11. This result due to the area of the stagnation continues to widen as the angle of attack increases. The effect of airflow speed towards drag coefficient can be seen in Figure 12. Higher the airflow speed create smaller drag coefficient value. At 12 m/s the C_D is 0.066 and at 26 m/s is 0.063.

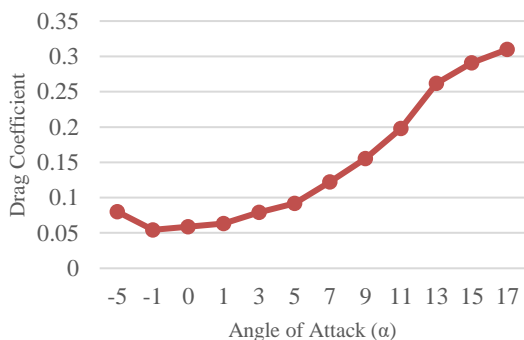


Fig. 11. C_D curve at 26 m/s



Fig. 12. The effect of airflow on C_D

The obtained moment coefficient curve tends to decline, in this case negative (-). Which means that the aircraft has the stability in flying conditions. Because for the stability of the plane, the value of C_M is a counter (inverse) from the addition of degrees of angle of attack. So that if α increases, the moment that occurs is the opposite and shows stability when flying. As shown in Figure 13. the moment coefficient at the Angle of Attack -5° is 0.053 and the Angle of Attack 17° is -0.0743.

The amount of pressure below the wing increases as the Angle of Attack increases. However, as shown in the curve, the amount of pressure decreases at the angle of attack of 15° . This shows that the plane experiences a stall condition due to reduced pressure that drives the aircraft to fly. We can also see in Figure 14. that the difference in mean pressure also occurs at different speeds. Where at 10° Angle of Attack with a speed of 16 m/s there is a pressure of 44.15 Pa, while at a speed of 26 m/s there is a pressure of 92.64 Pa. Meanwhile, below the Horizontal Elevator there is an increasing trend with increasing Angle of Attack.

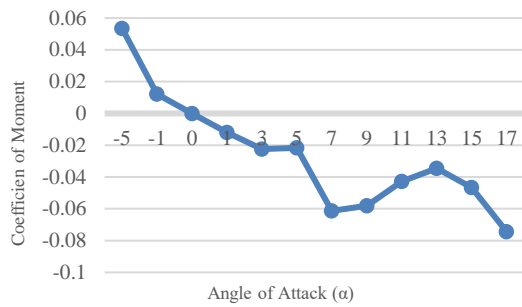


Fig. 13. Angle of attack effect on C_M at 26 m/s

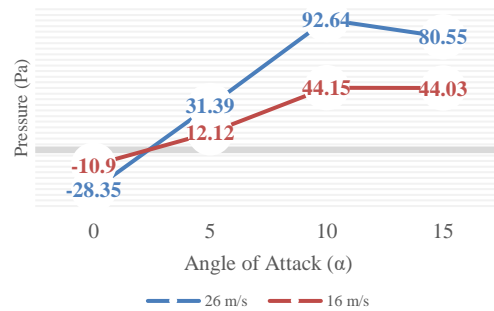


Fig. 14. Pressure distribution under wing

In the Figure 15 and Figure 16, as can be seen that the amount of pressure that occurs on the wing surface has decreased from the profile line position of -200 mm on the z axis to -600 mm on the z axis. This shows the amount of pressure in the wing area closer to the fuselage is greater than the wing area closer to the wingtip. This is due to the larger wing area in the area near the fuselage compared to the area around the wingtip, this makes direct contact to the airflow to be larger, so that the pressure that occurs is also bigger. It can be noted that the aircraft design has a strong wing structure, especially the joint area of the wing and fuselage.

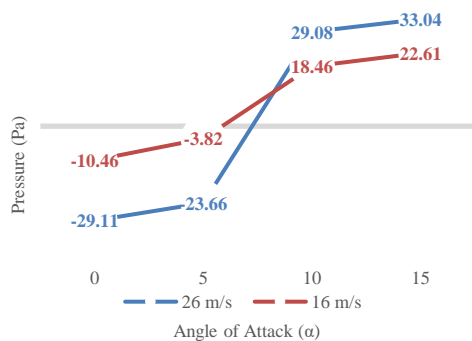


Fig. 15. Pressure profile below the H. elevator

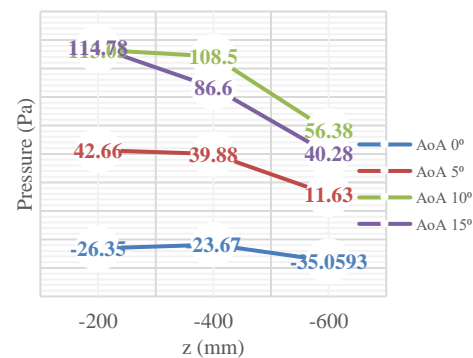


Fig. 16. Pressure profile on V-2 wing at 26 m/s

4. Conclusion

The results obtained from the numerical simulations using ANSYS Fluent has demonstrated its capability to obtain results similar to the wind tunnel results. The ANSYS Fluent provides results that enable researcher to save enormous cost in comparison to wind tunnel test. Several highlights of the simulation results were shown below

- i. At speed of 26 m/s, the Serindit V-2 aircraft has a maximum lift coefficient of 1.445086 at an angle of attack of 11°. And the stall angle occurs at an angle of 13° with a lift coefficient of 1.445086. The trend of the Drag Coefficient curve graph is incline, which mean it continues to increase as the angle of attack increases. The value of $C_D = 0.058912173$ and the highest is at the angle of attack of 17°, namely $C_D = 0.3099158$. Meanwhile, the C_M value tends to decrease. In this case it is negative, which means that the aircraft is stable in flying conditions. At the angle of attack 0° the C_M value obtained is -0.033237812. And also, at the angle of attack of 14° there is an increase in the curve where the C_M value is -0.12745846.
- ii. The amount of pressure below the wing and the horizontal of the elevator increases with increasing angle of attack and air flow velocity. The highest pressure occurs in the area closest to the fuselage.

References

- [1] Sadraey, Mohammad H. *Design of Unmanned Aerial Systems*. John Wiley & Sons, 2020. <https://doi.org/10.1002/9781119508618>
- [2] Dündar, Özgür, Mesut Bilici, and Tarik Ünler. "Design and performance analyses of a fixed wing battery VTOL UAV." *Engineering Science and Technology, an International Journal* 23, no. 5 (2020): 1182-1193. <https://doi.org/10.1016/j.jestch.2020.02.002>
- [3] Yunus, A. Cengel. *Fluid Mechanics: Fundamentals And Applications (Si Units)*. Tata McGraw Hill Education Private Limited, 2010.
- [4] Anuar, Kaspul, Musthafa Akbar, Hanif Abdul Aziz, and Agung Soegihin. "Experimental Test on Aerodynamic Performance of Propeller and Its Effect on The Flight Performance of Serindit V-2 UAV." *Journal of Advanced Research in Fluid Mechanics and Thermal Sciences* 91, no. 2 (2022): 120-132. <https://doi.org/10.37934/arfmts.91.2.120132>
- [5] Fahlstrom, Paul, and Thomas Gleason. *Introduction to UAV systems*. John Wiley & Sons, 2012. <https://doi.org/10.1002/9781118396780>
- [6] Austin, Reg. *Unmanned aircraft systems: UAVS design, development and deployment*. John Wiley & Sons, 2011. <https://doi.org/10.1002/9780470664797>
- [7] Anuar, K., and M. Akbar. "Wing design of uav serindit v-1." In *IOP Conference Series: Materials Science and Engineering*, vol. 539, no. 1, p. 012002. IOP Publishing, 2019. <https://doi.org/10.1088/1757-899X/539/1/012002>
- [8] Kharulaman, Liyana, Abdul Aabid, Fharukh Ahmed Ghasi Mehaboobali, and Sher Afghan Khan. "Research on Flows for NACA 2412 Airfoil using computational fluid dynamics method." *Int. J. Eng. Adv. Technol* 9, no. 1 (2019): 5450-5456. <https://doi.org/10.35940/ijeat.A3085.109119>
- [9] Lee, D., Taku Nonomura, Akira Oyama, and Kozo Fujii. "Comparative studies of numerical methods for evaluating aerodynamic characteristics of two-dimensional airfoil at low Reynolds numbers." *International Journal of Computational Fluid Dynamics* 31, no. 1 (2017): 57-67. <https://doi.org/10.1080/10618562.2016.1274398>
- [10] Povitsky, Alex, and Kristopher C. Pierson. "Vorticity Confinement Applied to Accurate Prediction of Convection of Wing Tip Vortices and Induced Drag." *International Journal of Computational Fluid Dynamics* 35, no. 3 (2021): 143-156. <https://doi.org/10.1080/10618562.2020.1856822>
- [11] Hossain, S., Muhammad Ferdous Raiyan, Mohammed Nasir Uddin Akanda, and Nahed Hassan Jony. "A comparative flow analysis of NACA 6409 and NACA 4412 aerofoil." *International Journal of Research in Engineering and Technology* 3, no. 10 (2014): 342-350. <https://doi.org/10.15623/ijret.2014.0310055>
- [12] Gan, Edwin Chern Junn, Mikhail Fong, and Yee Luon Ng. "CFD Analysis of Slipstreaming and Side Drafting Techniques Concerning Aerodynamic Drag in NASCAR Racing." *CFD Letters* 12, no. 7 (2020): 1-16. <https://doi.org/10.37934/cfdl.12.7.116>
- [13] Saroinsong, Hardy S., Vecky C. Poekoel, and Pinrolinvic D. Manembu. "Rancang Bangun Wahana Pesawat Tanpa Awak (Fixed Wing) Berbasis Ardupilot." *Jurnal Teknik Elektro dan Komputer* 7, no. 1 (2018): 73-84.
- [14] Kostić, Čedomir, Aleksandar Bengin, Boško Rašuo, and Dijana Damljanović. "Calibration of the CFD code based on testing of a standard AGARD-B model for determination of aerodynamic characteristics." *Proceedings of the Institution of Mechanical Engineers, Part G: Journal of Aerospace Engineering* 235, no. 10 (2021): 1129-1145. <https://doi.org/10.1177/0954410020966859>
- [15] Ma, Yang, Wei Zhou, Qilong Han, and Xueren Wang. "Aerodynamic configuration of the HCW based on the lifting body." *Journal of Aerospace Engineering* 32, no. 2 (2019): 04019004. [https://doi.org/10.1061/\(ASCE\)AS.1943-5525.0000950](https://doi.org/10.1061/(ASCE)AS.1943-5525.0000950)
- [16] Khan, Sher Afghan, Musavir Bashir, Maughal Ahmed Ali Baig, and Fharukh Ahmed Ghasi Mehaboob Ali. "Comparing the effect of different turbulence models on the CFD predictions of NACA0018 airfoil aerodynamics." *CFD Letters* 12, no. 3 (2020): 1-10. <https://doi.org/10.37934/cfdl.12.3.110>
- [17] Khan, Sher Afghan, Abdul Aabid, and C. Ahamed Saleel. "CFD simulation with analytical and theoretical validation of different flow parameters for the wedge at supersonic Mach number." *International Journal of Mechanical and Mechatronics Engineering* 19, no. 1 (2019): 170-177.
- [18] Dantsker, Or, and Moiz Vahora. "Comparison of Aerodynamic Characterization Methods for Design of Unmanned Aerial Vehicles." In *2018 AIAA Aerospace Sciences Meeting*, p. 0272. 2018. <https://doi.org/10.2514/6.2018-0272>
- [19] Hamizi, Ilya Bashiera, and Sher Afghan Khan. "Aerodynamics investigation of delta wing at low Reynold's number." *CFD Letters* 11, no. 2 (2019): 32-41.
- [20] Romadhon, Awal, and Dana Herdiana. "Analisis Cfd Karakteristik Aerodinamika Pada Sayap Pesawat Lsu-05 Dengan Penambahan Vortex Generator (Analysis of Cfd Aerodynamic Characteristics At the Wing of Aircraft Lsu-05 With the Addition of Vortex Generator)." *Jurnal Teknologi Dirgantara* 15, no. 1 (2017): 45-58. <https://doi.org/10.30536/j.jtd.2017.v15.a2518>